Structural and Biochemical Characterization of the Oxidoreductase NmDsbA3 from *Neisseria meningitidis**

Julian P. Vivian[‡1,2], Jessica Scoullar[§1], Amy L. Robertson[‡], Stephen P. Bottomley[‡], James Horne[¶], Yanni Chin[¶], Jerome Wielens[¶], Philip E. Thompson[¶], Tony Velkov[¶], Susannah Piek[§], Emma Byres[‡], Travis Beddoe[‡3], Matthew C. J. Wilce[‡], Charlene M. Kahler[§4,5], Jamie Rossjohn[‡4,6], and Martin J. Scanlon[¶4,7]

From [‡]*The Protein Crystallography Unit, ARC Centre of Excellence in Structural and Functional Microbial Genomics, School of Biomedical Sciences, Monash University, Clayton, Victoria 3800, the* [§]*School of Biomedical, Biomolecular & Chemical Sciences, QEII Medical Centre, University of Western Australia, Crawley, Western Australia 6009, and the* [¶]*Medicinal Chemistry and Drug Action, Monash Institute of Pharmaceutical Sciences, Monash University (Parkville Campus), 381 Royal Parade, Parkville, Victoria 3052, Australia*

DsbA is an enzyme found in the periplasm of Gram-negative bacteria that catalyzes the formation of disulfide bonds in a diverse array of protein substrates, many of which are involved in bacterial pathogenesis. Although most bacteria possess only a single essential DsbA, *Neisseria meningitidis* is unusual in that it possesses three DsbAs, although the reason for this additional redundancy is unclear. Two of these *N. meningitidis* enzymes (NmDsbA1 and NmDsbA2) play an important role in meningococcal attachment to human epithelial cells, whereas NmDsbA3 is considered to have a narrow substrate repertoire. To begin to address the role of DsbAs in the pathogenesis of *N. meningitidis*, we have determined the structure of NmDsbA3 to 2.3-Å resolution. Although the sequence identity between NmDsbA3 and other DsbAs is low, the NmDsbA3 structure adopted a DsbA-like fold. Consistent with this finding, we demonstrated that NmDsbA3 acts as a thiol-disulfide oxidoreductase *in vitro* and is reoxidized by *Escherichia coli* DsbB (EcDsbB). However, pronounced differences in the structures between DsbA3 and EcDsbA, which are clustered around the active site of the enzyme, suggested a structural basis for the unusual substrate specificity that is observed for *Nm*DsbA3.

Neisseria meningitidis, the causative agent of epidemic meningitis, is a significant public health burden worldwide causing 1.2 million cases per year globally, with an estimated fatality rate of 10% (WHO) (1). The disease is difficult to diagnose in the clinic because onset symptoms are similar to influenza, and delays in the administration of antibiotics has been directly correlated with death of the patient, since the rapid progression of the disease from bacteremia and/or meningitis to life threatening septic shock syndrome can occur within the first few hours after the initial symptoms appear. Because of these parameters, vaccination is the preferred option for the control of this disease in the community. Meningococci express one of five capsular serogroups (A, B, C, W-135, and Y) and successful vaccines based upon four of these polysaccharides are available (1). There is no vaccine candidate for serogroup B isolates as this capsular type mimics human antigens and is therefore a poor immunogen. As a consequence there is still considerable interest in examining the pathogenic mechanisms of this organism as this knowledge may lead to an improved understanding of the development of infection and disease, which may provide novel avenues to treatment.

To initiate disease, *N. meningitidis* must invade non-ciliated cells of the mucosal epithelium lining the human nasopharynx, translocate into the subepithelial tissue, and gain access to the bloodstream (2). In this compartment, the bacteria grow to high density ultimately resulting in the clinical syndrome of septic shock (3). A diverse array of virulence factors have been implicated in this process (3) including thiol-disulfide oxidoreductases of the Dsb family (4).

The Dsb family of proteins are oxidoreductases that were initially identified in the periplasm of Gram-negative bacteria (5–10). The family is responsible both for introducing disulfide bonds into nascent polypeptides in the periplasm and, where necessary, for reshuffling incorrectly formed disulfides to enable productive protein folding. There are several members of the Dsb family with distinct roles: DsbA catalyzes the oxidation of a wide range of substrate proteins via an efficient thiol-disulfide transfer mechanism.

Many of the DsbA substrates are involved in bacterial pathogenesis. Reduced DsbA, which is formed in the reaction, is reoxidized by a membrane-bound partner, DsbB. DsbA/B form the oxidative system that is primarily responsible for the forma-

tion of new disulfide bonds in substrates within the periplasm. For substrates that contain more than one pair of cysteine residues, there exists the possibility that disulfides may be linked incorrectly by DsbA, hence a second, complementary system exists to catalyze disulfide isomerization; DsbC and its membrane-bound reductive partner DsbD (Ref. 11, and references therein).

Interestingly, most Gram-negative organisms possess only a single DsbA and inactivation of the gene results in complete loss of virulence. This has been ascribed to the loss of function and increased degradation rates of misfolded substrates of DsbA (12, 13). The Dsb system of *Escherichia coli* is the best characterized and is widely used as a paradigm for the Dsb systems of other Gram-negative bacteria. In *E. coli*, there is a single DsbA enzyme (EcDsbA), which is responsible for oxidation of a diverse array of protein substrates. *E. coli* express several hundred potential DsbA substrates, *i.e.* proteins that are predicted to enter the periplasm and contain at least one pair of cysteine residues (14). Typically *dsbA*-null *E. coli* show reduced levels of proteins that contain disulfides (6), including enzymes such as alkaline phosphatase (AP)[8] as well as outer membrane flagellar motor proteins (12). The latter renders *dsbA*-null *E. coli* non-motile.

In contrast, bioinformatic analysis suggests that *N. meningitidis* has fewer potential DsbA substrates, but unusually, it possesses three chromosomally encoded oxidoreductases, NmDsbA1, NmDsbA2, and NmDsbA3. NmDsbA1 and NmDsbA2 share 78% amino acid identity, are lipoproteins that are anchored in the periplasmic membrane, and are both necessary for the formation of "functional" Type IV pili (4). NmDsbA1/NmDsbA2 double mutants express intact pilin fibers, but are deficient in attachment to cell lines. In addition, they have decreased transformation rates, which has been ascribed to a reduction in the level of expression of functional PilQ, the outer membrane porin through which the Type IV pili are extruded (15). It has been demonstrated that NmDsbA3, which is not membrane anchored and has 57 and 51% sequence identity with NmDsbA1 and NmDsbA2, respectively, is unable to compensate for the loss of NmDsbA1/2. The ability of each of the Neisserial DsbA enzymes to complement *dsbA*-null *E. coli* has also been tested (16). Although NmDsbA1 restored motility, NmDsbA2 and NmDsbA3 did not (16). In contrast, EcDsbA and NmDsbA2 were able to fully restore AP activity in *dsbA*-null *E. coli* to wild type levels, NmDsbA1 partially restored AP activity and NmDsbA3 had no effect on AP activity (16).

These observations suggest that the meningococcal oxidoreductases display preferred substrate recognition patterns and therefore are likely to be involved in multiple and distinct processes of meningococcal pathogenesis. To begin to define the role of the *Neisserial* DsbA oxidoreductases in meningococcal pathogenesis and establish the basis for separate substrate specificities for these enzymes, we have determined the 2.3-Å

resolution structure of NmDsbA3. In addition we have determined the oxidoreductase activity of NmDsbA3 both *in vitro* and *in vivo*. These findings suggest that NmDsbA3 functions as a disulfide oxidase, but that differences in the active site correlate with its limited substrate repertoire. Collectively, these studies suggest a structural basis for substrate specificity in the DsbA family in *N. meningitidis*.

EXPERIMENTAL PROCEDURES

Bacterial Strains, Plasmids, and Culture Conditions

E. coli strain JM109 was used as the recipient for cloning experiments, whereas *E. coli* strains JCB570 and JCB571 (kindly provided by James Bardwell, University of Michigan) were used for complementation assays. *E. coli* strains were grown aerobically in Luria-Bertani (LB) broth (1% tryptone, 0.5% yeast extract, 0.5% NaCl (w/v)) at 37 °C with shaking (220 rpm) or on LB containing 1% agar (w/v). The growth medium was supplemented with ampicillin (50 μg/μl), chloramphenicol (30 μg/μl), isopropyl 1-thio-β-D-galactopyranoside (0.3 mM), or 5-bromo-4-chloro-3-indolyl-β-D-galactopyranoside (X-gal) (20 μg/ml) as required.

Recombinant DNA Techniques

Unless otherwise stated recombinant standard DNA techniques were used throughout (17). Plasmid extractions were conducted using the High Pure Plasmid Isolation Kit (Roche Applied Sciences), whereas PCR products were purified using Qiagen PCR purification kit. Sterile H_2O supplemented with 1 M Tris buffer (pH 8.0) was used in place of the commercial elution buffer in both kits. Yield and quality of DNA was determined by agarose gel electrophoresis.

The *N. meningitidis dsbA3* gene was amplified from *N. meningitidis* strain MC58 using DAP103 (5′-catgccatggcgaaaggaaataattatgaagctc-3′) and DAP104 (5′-catgccatggcttgcgcttcttcggatacg-3′), whereas the *E. coli dsbA* was amplified from *E. coli* strain JM109 using KAP13 (5′-catgccatgggagccgactttatagaacaggc-3′) and KAP14 (5′-gctctagagaaataatgtccagcggcaggatgc-3′). The amplified fragments were cloned into the low copy expression vector pHSG576 to create plasmids pJKD2719 containing *NmdsbA3* and pCMK255 containing *EcdsbA*, respectively. The *NmdsbA3*, and *EcdsbA* genes were excised by flanking NcoI sites from pJKD2719 and pCMK255, respectively, and cloned into the high copy expression vector pTrc99A to create plasmids pJKD2645 and pCMK268. Inserts were confirmed by sequencing on an ABI Prism 3730 48 capillary automated DNA sequencer using primers KAP96 (5′-agcggataacaatttcacacagga-3′) and KAP97 (5′-gttttcccagtcacgac-3′) or DAP381 (5′-gagcggataacaatttcacacagg-3′) and DAP382 (5′-cgtgcacccaactgatcttcagc-3′) as appropriate. Plasmids pHSG576 (18), pCMK255, and pJKD2719 were transformed into the *E. coli dsbA* mutant strain JCB571 as described previously (19) creating strains CKEC271, CKEC272, and CKEC276. Plasmids pTrc99A, pCMK268, and pJKD2645 were transformed into the *E. coli dsbA* mutant strain JCB571 creating the strains CKEC288, CKEC289, and CKEC293, respectively.

NmDsbA3 with an N-terminal His fusion was created by SOE-PCR. The His-enterokinase cleavage site fragment was amplified from expression vector pET45b(+) (Invitrogen) using primers

---

[8] The abbreviations used are: AP, alkaline phosphatase; EcDsb, *Escherichia coli* Dsb; NmDsb, *Neisseria meningitidis* Dsb; DTT, dithiothreitol; HPLC, high performance liquid chromatography; LC, liquid chromatography; MS, mass spectrometry; VcDsbA, *Vibrio cholerae* DsbA.

KAP159 (5′-gactcactataggggaattgtgagc-3′) and KAP167 (5′-ggcatacttgtcgtcgtcatcattcgaacc-3′). The NmDsbA3 gene was amplified from NMB chromosomal DNA with primers KAP166 (5′-gacaagtatgccctgacggaaggggaagac-3′) and DAP269 (5′-cccaagcttggcaaacactaccgccaaaactgc-3′). Primers KAP167 and KAP166 contained complementary sequences that allowed PCR amplification of both fragments in a second round PCR with primers KAP161 (5′-ggaattgtgagcggataacaattccc-3′) and KAP168 (5′-gcaagcttctatttctgtacagcaggggtctgac-3′). This PCR fragment was then digested with HindIII and cloned into the HindIII site of expression vector pET45b(+) to create the expression vector pCMK140.

Protein Expression and Purification

EcDsbA was expressed and purified as described previously (20). His$_6$-tagged NmDsbA3 was expressed in BL21 C43 cells using autoinduction (21). Briefly, cells harboring pET45b-NmDsbA3 were grown with agitation at 200 revolutions min^{-1} for 48 h at 293 K in minimal medium (21) supplemented with ampicillin (100 μg ml^{-1}). Cells were harvested by centrifugation and lysed using Bugbuster^{TM} (Novagen) according to the manufacturers instructions. The cleared lysate was applied to a nickel-nitrilotriacetic acid resin (GE Healthcare) and washed with a buffer containing KH$_2$PO$_4$ (10 mM), NaCl (300 mM), and imidazole (20 mM) (pH 8.0) and eluted on a gradient from 20 to 500 mM imidazole. Fractions were analyzed by SDS-PAGE and those containing NmDsbA3 were concentrated and buffer exchanged using an Amicon 5000 MWCO spin concentrator (Millipore) into HEPES (10 mM) (pH 6.8). The resulting solution was applied to a cation exchange column (Mono S HR 5/5, GE Healthcare) and NmDsbA3 eluted on a NaCl gradient (0–250 mM) in buffer B. NmDsbA3 was chemically oxidized (1.7 mM copper(II) phenanthroline) or reduced (10 mM dithiothreitol). Oxidizing or reducing agents were removed by gel filtration (Superdex 75, GE Healthcare) in Buffer C (10 mM HEPES, pH 6.8, 150 mM NaCl).

Native NmDsbA3 protein for crystallographic studies was expressed in *E. coli* BL21 DE3 Codon Plus cells (Stratagene) transformed with pJKD2645. Cells were grown at 37 °C in Luria-Bertani medium containing ampicillin (100 μg ml^{-1}) until an optical density at 600 nm of 0.6 was reached. Cultures were induced by adding 1 mM isopropyl 1-thio-β-D-galactopyranoside, grown for a further 5 h, and harvested by centrifugation. Periplasmic proteins were released by resuspending the cell pellet in 10 mM HEPES (pH 7.8), 150 mM NaCl containing polymyxin B sulfate (1 mg ml^{-1}) for 2 h at room temperature. The resulting cultures were clarified (16,000 × *g* for 30 min) and purified chromatographically. In the first step, ammonium sulfate (1 M) was added to the periplasmic extract, which was filtered and applied to a hydrophobic interaction column (Phenyl HP 16/10 column (GE Healthcare). Proteins were eluted on an ammonium sulfate gradient (1 → 0 M) in 10 mM HEPES (pH 7.8), 150 mM NaCl. Fractions were analyzed by SDS-PAGE and those containing NmDsbA3 were pooled and diafiltered (Amicon Ultra 5, Millipore) into 10 mM HEPES (pH 6.8). The protein was purified further using MonoS and gel filtration as described above. Selenomethionine-labeled NmDsbA3 was expressed from *E. coli* B384 in minimal media containing selenomethio-

nine using the protocol described by Marley *et al.* (22). The protein was purified as described above and concentrated to 20 mg ml^{-1} for crystallization.

Crystallization and X-ray Diffraction Data Collection

Selenomethionine-labeled NmDsbA3 was crystallized using the hanging-drop vapor-diffusion method. 1 μl of protein solution was mixed with 1 μl of precipitant solution (20% PEG 4000, 0.1 M Tris, pH 8.0, 0.2 M sodium acetate) and incubated at 294 K. Crystals appeared within 4 days and grew as thin plates to dimensions 0.4 × 0.1 × 0.05 mm. The crystals were mounted in nylon loops and passed through a solution of mother liquor plus 20% (v/v) glycerol prior to flash-cooling in a nitrogen stream at 100 K. X-ray diffraction data were collected at wavelengths corresponding to the peak (0.97939 Å) and inflection (0.97952 Å) of the selenium absorption edge and at a remote wavelength (0.97242 Å). 360° of data were collected for each wavelength with 0.5° oscillations at beamline 23ID-B GM/CA of the Advanced Photon Source, Argonne National Laboratories, from a single crystal mounted 260 mm from a Quantum 4 CCD detector. The crystal was of space group $P2_1$, with unit cell dimensions $a = 54.5$ $b = 88.6$ $c = 84.4$ Å, $\beta = 106.9°$ and diffracted to beyond 2.3 Å. The data were processed and scaled with DENZO (23) and SCALEPACK (23). Due to significant radiation damage to the crystal only the peak wavelength was used for subsequent structural determination. The data collection statistics of the peak wavelength are summarized in Table 1.

Structure Determination and Refinement

MAD phasing was pursued as earlier attempts at molecular replacement using related DsbA structures in the Protein Data Bank were unsuccessful. Due to radiation damage to the crystal the inflection and remote wavelength datasets were ignored and a SAD phasing approach using only the peak wavelength dataset to a maximum resolution of 3.0 Å was employed. SOLVE (24) was used to determine the positions of the 16 selenium atoms and subsequent density modification was performed by RESOLVE (24). Visual inspection of the modified electron density map revealed that each of the 4 copies of NmDsbA3 adopted a DsbA-like fold. The four molecules of NmDsbA3 in the asymmetric unit were arranged as a crystallographic tetramer, although there is no evidence for DsbA3 acting as a physiological tetramer and moreover DsbA3 behaved as a monomer on gel filtration. In this crystallographic tetrameric arrangement the catalytic cysteines at position 37 were within 5 Å of their non-crystallographically related symmetry equivalents. However, there was no continuous electron density observed indicative of the presence of intermolecular disulfide bonds. This is consistent with DsbA3 being in its reduced state.

MOLREP (25, 26) was thus used to place 4 copies of TcpG (27) (PDB accession code 1BED) into the modified electron density map. The model was improved by iterative rounds of manual building in COOT (28) and maximum-likelihood based refinement in REFMAC, with TLS (25, 29). Strict NCS restraints were applied in the early rounds of refinement and were subsequently loosened and then removed for the final round of refinement. Solvent molecules were added with COOT and checked by visual inspection of $F_o − F_c$ maps. The

structure was validated using the Ramachandran plot, density fit, rotamer, and geometry analysis as implemented in COOT. Manual model building was continued until no peaks greater or less than 4σ were present in a $F_o - F_c$ difference Fourier electron density map. The refinement statistics are summarized in Table 1. The final coordinates have been deposited in the Protein Data Bank under accession code 2ZNM.

Insulin Reduction Assay

Oxidoreductase activity was measured by following the rate of precipitation of the insulin B chain from solution in the presence of dithiothreitol (DTT) (30). Reactions were performed in 10 mM HEPES (pH 7.8), 150 mM NaCl containing 1 mM EDTA. The reaction mixtures contained insulin (100 μM) plus either EcDsbA or His$_6$-NmDsbA3 (5 μM). The reaction was initiated by addition of DTT (2 mM) and the rate of precipitation was monitored from the increased turbidity of the reaction mixture, which was measured as the absorbance at 650 nm. Absorbance measurements were made in a 1-cm cell using a Cary50 spectrophotometer (Varian). The rate of insulin reduction by DTT in the absence of DsbA was measured as a control.

Reoxidation of DsbA by EcDsbB

The reoxidation of EcDsbA and His$_6$-NmDsbA3 by EcDsbB was measured as previously described (31). An EcDsbB overproducing strain, JCB851, was a kind gift from James Bardwell (University of Michigan). EcDsbB was expressed and purified as previously described (31). Oxidation of DsbA was detected by following the time dependent change in intrinsic tryptophan fluorescence that accompanies formation of the disulfide bond in DsbA. EcDsbA and NmDsbA3 exhibit similar fluorescence properties, with the reduced form of the protein having significantly higher fluorescence in each case. Fluorescence was measured on a Cary Eclipse fluorimeter (Varian) using an excitation wavelength of 295 nm and a detection wavelength of 330 nm. 5-nm slit widths were used for both excitation and emission and the temperature was maintained at 30 °C with a Peltier-controlled cell holder. DsbA was reduced immediately prior to the assay with DTT (10 mM). The DTT was removed by gel filtration in Buffer E (50 mM sodium phosphate, pH 8.0, 150 mM NaCl, 0.1% dodecylmaltoside containing 1 mM EDTA (to prevent aerial oxidation of DsbA)) (Superdex 75, GE Healthcare). Reduced and oxidized EcDsbB have identical intrinsic fluorescence (31), hence the oxidation state of EcDsbB does not contribute to the observed changes.

Kinetics of Oxidation of Substrate Peptide

Disulfide oxidase activity was measured by following the change in the intrinsic fluorescence of each DsbA upon oxidation of a peptide substrate. The substrate peptide was derived from the mature sequence of the meningoccol *pilE2* protein. Synthesis of the acetylated peptide Ac-C(Trt)-Q(Trt)-K(Boc)-G-D(OtBu)-G-T(tBu)-K(Boc)-N(Trt)-Ser(tBu)-C(Trt)-RESIN, was performed on Rink resin under standard solid phase peptide synthesis conditions. Final cleavage and deprotection was carried out using 95% (v/v) trifluoroacetic acid. The product was recovered by a standard sequence of ether precipitation, dissolution in 50% (v/v) aqueous acetonitrile, freeze drying followed by HPLC purification and the peptide sequence confirmed by LC-MS. The kinetics of oxidation of the substrate peptide PilE2, by His$_6$-NmDsbA3 and EcDsbA were determined in buffer C using an Applied Photophysics SF.18MV stopped-flow apparatus, thermostatted at 20 °C. Peptide oxidation was followed by monitoring the change in intrinsic fluorescence of the DsbA variants upon reduction at wavelengths >320 nm (λ_{ex} = 280 nm). A 10-fold molar excess of peptide substrate was used, such that the final concentration of the DsbA variant and peptide were 1 and 10 μM, respectively. Data were fit to a single exponential kinetic model for substrate peptide oxidation rate determination. The oxidation state of the peptide following the reaction with DsbA was determined using LC-MS. For comparison, samples of oxidized and reduced peptide were generated via chemical oxidation with copper phenanthroline (15 mM) or reduction with DTT (100 mM). DsbA in buffer C was added to the reduced peptide at molar ratios between 1:20 and 1:1 of DsbA:peptide. The mixtures were separated by reversed-phase chromatography on an Agilent 1100 HPLC using an Agilent Eclipse C18 column on a gradient from 0 to 40% acetonitrile in 0.1% formic acid over 20 min. Chromatographic separation was monitored by recording the total ion current and the mass of the peptides in the resulting peaks was analyzed using Agilent 6510 Q-TOF mass spectrometer.

Functional Analysis of DsbA Activity

DTT Sensitivity Assays—DTT assays were carried out as previously described (32). Briefly, strains were grown in LB broth to mid-log phase, standardized to 2×10^8 cells/ml and diluted 10^{-1}, 10^{-2}, 10^{-3}, and 10^{-4}. Freshly prepared LB agar with and without DTT (15 mM) was drop inoculated with each dilution (5 μl) and incubated at 37 °C for 18 h.

Motility Assays—Motility assays were performed essentially as described (33). Briefly, strains were grown in LB broth to mid-log phase and standardized to 2×10^8 cells/ml. Freshly prepared soft LB agar (0.4%) plates were drop inoculated with culture dilution (5 μl) and swarming was observed after overnight incubation at 37 °C.

RESULTS

Structure of NmDsbA3—To gain insight into the function of NmDsbA3, we expressed, purified, crystallized, and determined its structure in its reduced state using the single wavelength anomalous diffraction method and refined the structure to 2.3-Å resolution to R_{factor} and R_{free} values of 21.0 and 26.3%, respectively (Table 1). There are four molecules of NmDsbA3 in the asymmetric unit, all of which are highly similar (root mean square deviation of 0.2–0.5 Å over Cα atoms). Accordingly, one monomer in the asymmetric unit has been used throughout for subsequent analyses. The structure revealed that NmDsbA3 adopted a canonical DsbA-fold (34), containing a thioredoxin domain that contains an inserted α-helical domain (Fig. 1). The classical thioredoxin fold comprises a four-stranded β-sheet that is flanked by three α-helices (35). NmDsbA3 contains an additional β-strand (β1 in Fig. 1) that precedes the N-terminal portion of the thioredoxin domain, which is formed by residues 23–61. These residues incorporate strand β2, helix α1, and strand β3 of NmDsbA3, which form the

Basis for Substrate Specificity in Meningococcal DsbA Enzymes

TABLE 1
X-ray data collection and processing statistics
Values in parentheses represent those of the highest resolution shell 2.38-2.30 Å.

Space group	$P2_1$
Cell dimensions (Å)	$a = 54.5\ b = 88.5\ c = 84.3,\ \beta = 106.9°$
Resolution (Å)	50-2.3
R_{sym}[a]	4.8 (27.8)
$I/\sigma I$	43.3 (5.0)
Completeness (%)	94 (65)
Redundancy	5.2
Refinement	
Resolution (Å)	30-2.3
Reflections in working set	34,110
R_{factor}[b]	0.210
R_{free}[b]	0.263
Total residues	
A chain	3–187
B chain	3–187
C chain	3–188
D chain	3–186
Total protein atoms	5,863
Total waters	176
Bond lengths (Å)	0.009
Bond angles (°)	1.197
Ramachandran analysis	
Most favored (%)	91.8
Additionally allowed (%)	8.2
Average B factor (Å²)	58.5

[a] $R_{sym} = \Sigma_h \Sigma_l |I_{hl} - \langle I(h) \rangle| / I_h \Sigma_l \langle I_h \rangle$, where I_{hl} is the lth observation of reflection **h** and $\langle I_h \rangle$ is the weighted average intensity for all observations l of reflection **h**.

[b] $R_{factor} = \Sigma_{hkl} \|F_o| - |F_c\| / \Sigma_{hkl} |F_o|$ for all data excluding the 5% that comprised the R_{free} used for cross-validation.
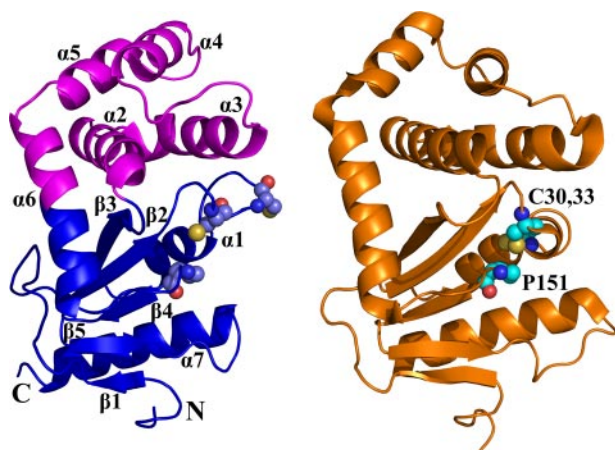

FIGURE 1. **Schematic representation of the structures of NmDsbA3 and EcDsbA.** *A*, NmDsbA3 adopts a canonical DsbA-fold comprising a thioredoxin domain (shown in *blue*) with an inserted α-helical domain (shown in *magenta*). The heavy atoms of the two cysteines and *cis*-Pro residue that form the conserved active site residues of the thioredoxin domain are shown as *spheres*. *B*, EcDsbA in the same orientation (Protein data bank code 1FVK; chain B). The heavy atoms of Cys30, Cys33, and *cis*-Pro151 in the active site are shown as *spheres*.
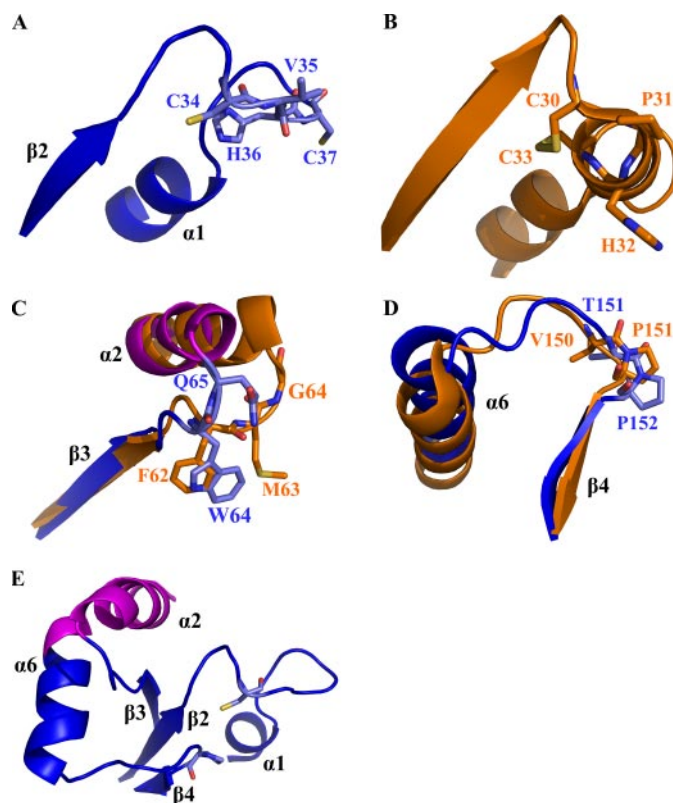

FIGURE 2. **Comparison of the structure of active site loops in NmDsbA3 and EcDsbA.** *A*, in NmDsbA3 the active site Cys34-Val-His-Cys37 forms an extended loop. *B*, the active site Cys30-Pro-His-Cys33 of EcDsbA forms the first turn of helix α1 in the thioredoxin domain. *C* and *D*, superposition of the loops connecting the thioredoxin and helical domains of NmDsbA3 and EcDsbA. Residues are colored as described in the legend to Fig. 1. Key amino acid residues are shown in *stick* representation and labeled. *E*, these regions of the structure form a contiguous surface that surrounds the active site of DsbA.

doxin domains. Accordingly, the structure of NmDsbA3 shared a number of structural features typified by the DsbA-fold.

Comparison with EcDsbA—To gain a more detailed understanding of the function of NmDsbA3, we next compared the structure to that of EcDsbA, which is the most thoroughly characterized member of the DsbA family. Whereas the sequence identity between NmDsbA3 and EcDsbA is only 24%, their structures can be superimposed with a root mean square deviation of 1.9 Å over 116 Cα atoms. Nevertheless, there are several differences between the two structures that appear to be functionally relevant. The most notable is the conformation of the active site C*XX*C motif. In NmDsbA3, the Cys34-Val-His-Cys37 motif is present on an extended loop that precedes the α1-helix (Fig. 2*A*). Whereas in EcDsbA, the active site is positioned at the N terminus of α1-helix, in which Cys30-Pro-His-Cys34 form the first turn of the helix (Fig. 2*B*). A second critical difference lies in the conformation of the loop that connects the β3-strand in the thioredoxin domain to the α2-helix in the helical domain (Fig. 2*C*). Here, a two-residue deletion in NmDsbA3 resulted in a significant change in the conformation of this loop. The third notable difference lay in the conformation of the loop (Fig. 2*D*), which connects α6-helix to the β4-strand of the thioredoxin domain and contains the conserved *cis*-Pro residue. Collectively, these three regions of DsbA form a contiguous surface (Fig. 2*E*) that encompass the active site of the thioredoxin domains (35).
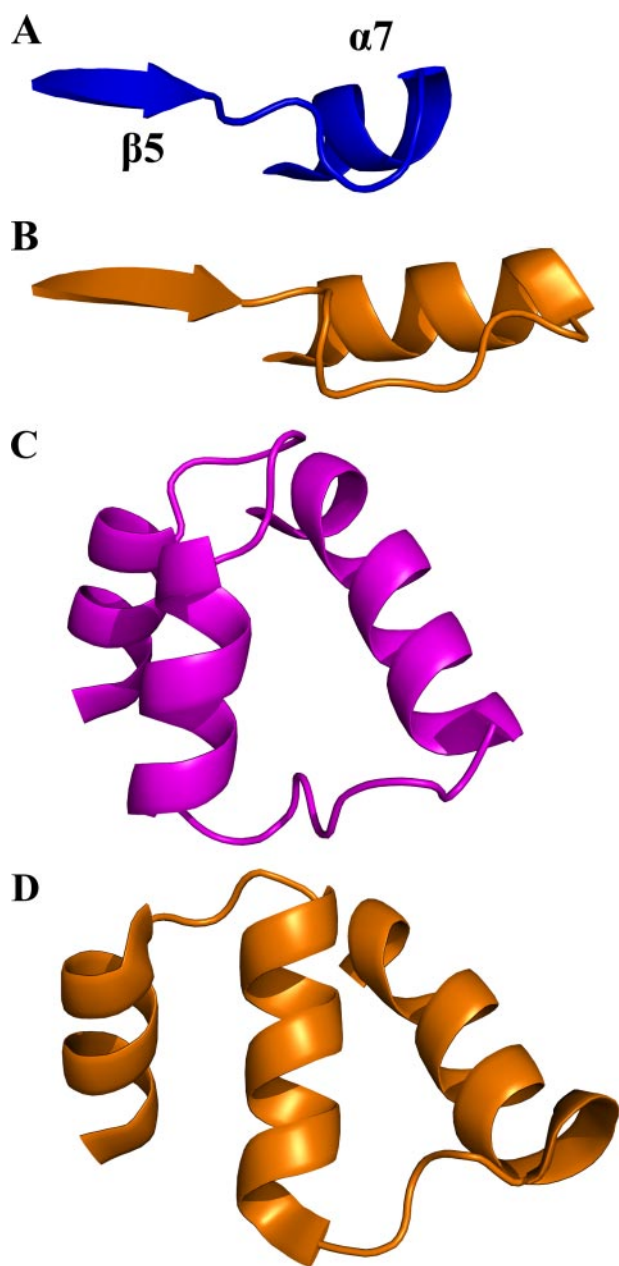
βαβ motif, including the active site C*XX*C sequence that is common to all thioredoxin-like proteins. The rest of the thioredoxin domain is formed by residues 140–186, incorporating the C-terminal portion of the long helix α6, strands β4 and β5, and helix α7, which form the remaining two α-helices and two β-strands in an αββα motif (35). This region of the protein includes the loop containing a *cis*-Pro residue that is located adjacent to the active site C*XX*C and is conserved in all thioredoxin-like proteins (Fig. 1*B*). The helical domain encompasses residues 66–139 and contains four helices (α2-α5) plus an extension of helix α6, which connects the helical and thiore-

FIGURE 3. **Differences in the structures of NmDsbA3 and EcDsbA.** *A* and *B*, helix α7, which forms a part of the hydrophobic groove that in EcDsbA is the binding site for EcDsbB, is shortened in NmDsbA3 by four residues. *C* and *D*, the helical domains of NmDsbA3 and EcDsbA exhibit identical topologies, although insertions and deletions in the loops between the helices result in displacement of their positions in the two structures.

In the helical domain of NmDsbA3, the loop between the α3- and α4-helices contains an additional four residues, which causes a displacement of helix α4 and helix α5 relative to EcDsbA (Fig. 3, *A* and *B*). Notwithstanding this difference, the topology of the helical domains of NmDsbA3 and EcDsbA is conserved between the two structures.

Finally, the loop linking the β5-strand to the α7-helix of the thioredoxin domain of NmDsbA3 is four residues shorter than in EcDsbA, which results in helix α7 having one less turn of helix in NmDsbA3 (Fig. 3, *C* and *D*). This helix forms part of the hydrophobic groove below the active site in DsbA enzymes that is the binding site for EcDsbB (36). Comparison of the electro-
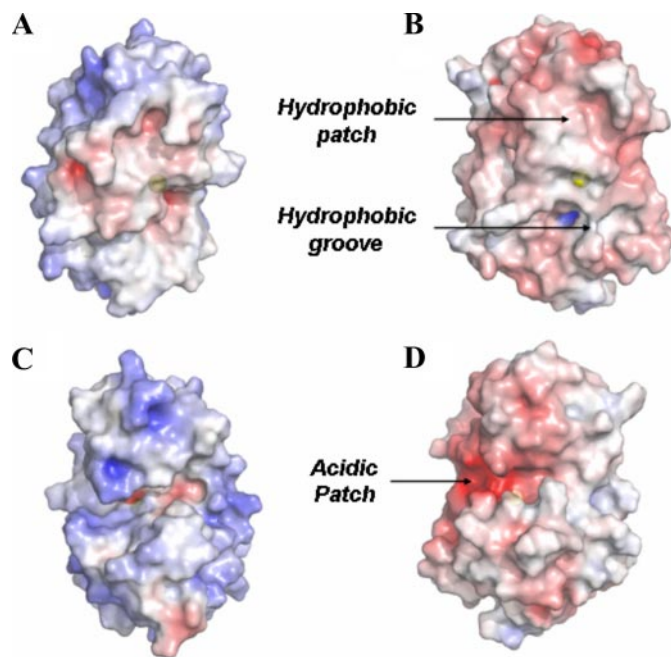

FIGURE 4. **Electrostatic surfaces of NmDsbA3 and EcDsbA.** Several of the hydrophobic surface features that surround the active site of EcDsbA (*B*) are conserved in NmDsbA3 (*A*). The hydrophobic groove in EcDsbA has been demonstrated as the site of interaction with DsbB. An acidic patch of residues that is present in EcDsbA (*D*) is absent in NmDsbA3 (*C*).

static surfaces of NmDsbA3 and EcDsbA (Fig. 4) revealed that NmDsbA3 retained the conserved hydrophobic features of the DsbB-binding site that have previously been observed in DsbA enzymes of Gram-negative bacteria (37).

In the structures of both EcDsbA and *Vibrio cholerae* DsbA (VcDsbA) (27, 34), there is a conserved acidic patch that is located on the face of the enzyme opposite the active site. Although no functional role has been ascribed to this region of the structure of DsbA, its conservation has led to the proposal that it may be functionally important (27). In NmDsbA3, there are no corresponding acidic residues in this region of the structure, and indeed NmDsbA3 is slightly basic in this region. The functional significance of this difference remains unresolved. Accordingly, whereas NmDsbA3 is similar to EcDsbA, there are a number of notable structural differences in the vicinity of the thioredoxin active site.

Disulfide Reductase Activity—Given that NmDsbA3 possessed a DsbA-fold, yet possessed unique features around the active site, we next tested the functional activity of NmDsbA3. The oxidoreductase activity of NmDsbA3 was characterized *in vitro*, first by determining its ability to reduce insulin. The insulin reduction assay follows precipitation of the insulin B-chain, which results from reduction of the interchain disulfide. The activity of NmDsbA3 was measured and compared with EcDsbA (Fig. 5*A*). Each increased the rate of precipitation over that caused by DTT alone in the absence of enzyme. The lag time to the appearance of measurable precipitate for NmDsbA3 was significantly longer than that observed for EcDsbA and the rate of precipitation was approximately halved. These observations are consistent with NmDsbA3 acting as a DsbA-like oxidase.
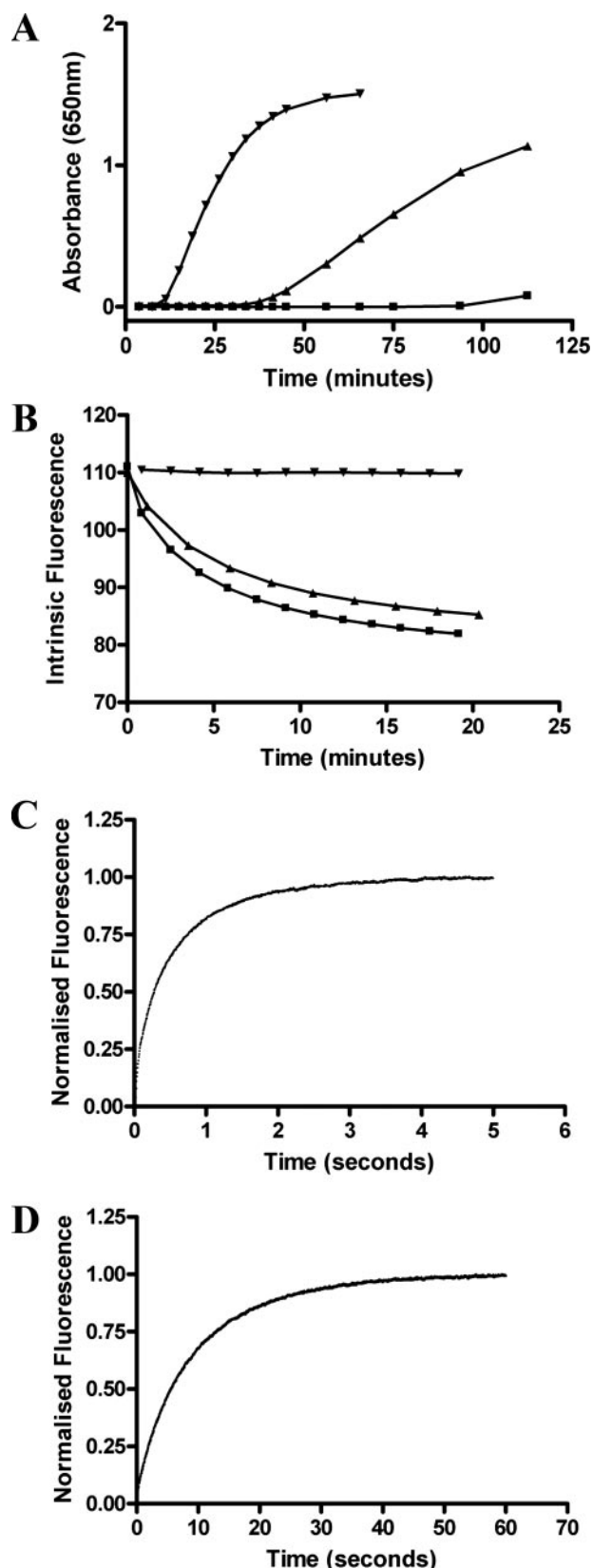
FIGURE 6. **HPLC-MS analysis of substrate peptide.** Chemically reduced (*A*) and oxidized (*B*) PilE2 peptide gave peaks with *m/z* 1181 and 1179, respectively, consistent with the presence of two free thiol groups in the reduced peptide and a disulfide in the oxidized peptide. *C*, addition of NmDsbA3 (1:20) to reduced PilE2 peptide resulted in the appearance of an earlier eluting peak in the chromatogram. *D*, analysis revealed that the new peak contained a species having *m/z* of 1179, indicating that reaction with NmDsbA3 resulted in formation of a disulfide in the PilE2 peptide.

Disulfide Oxidase Activity—Next, the disulfide oxidase activity was determined *in vitro* by measuring the rate of oxidation of a model substrate peptide. The sequence around the two cysteines in the major subunit of type IV *Neisserial* pili (PilE) was synthesized and used as a model substrate peptide. The kinetics of oxidation of the peptide by EcDsbA and NmDsbA3 were monitored by stopped-flow fluorescence. In each case the intrinsic fluorescence of the reduced form of DsbA was significantly higher than that of oxidized DsbA. In the course of the assay, oxidation of the peptide substrate resulted in concomitant reduction of the DsbA enzyme, which led to an increase in fluorescence. A 10-fold excess of peptide was used in the assay. The reactions showed first-order kinetics and the rate of oxidation of the PilE peptide substrate was somewhat slower in the case of EcDsbA ($k = 0.11$ s^{-1}) than NmDsbA3 ($k = 2.0$ s^{-1}) (Fig. 5, *C* and *D*). The peptide species generated by reaction with NmDsbA3 was analyzed by LC-MS (Fig. 6). This analysis revealed the reaction with NmDsbA3 generated a peptide with a shorter retention time on C18 reversed phase HPLC, which was 2 mass units lighter than the reduced peptide, consistent with formation of a disulfide bond in the reduced PilE2 peptide upon reaction with NmDsbA3. The oxidation of the peptide by NmDsbA3 was essentially quantitative. These data indicate that NmDsbA3 is capable of acting as a disulfide oxidase *in vitro*.

Reoxidation by EcDsbB—Next, the *in vitro* oxidation of reduced NmDsbA3 by *E. coli* EcDsbB was measured by recording the decrease in intrinsic fluorescence that accompanies oxi-

FIGURE 5. *In vitro* **activity of NmDsbA3.** *A*, disulfide reductase activity of NmDsbA3 was determined using the insulin reduction assay in the absence (■) and presence of (▼) EcDsbA (1 μM) or (▲) NmDsbA3 (1 μM). Both EcDsbA and NmDsbA3 catalyze the reduction of insulin by DTT. *B*, the ability of EcDsbB to reoxidize reduced DsbA was measured by following the decrease in intrinsic fluorescence that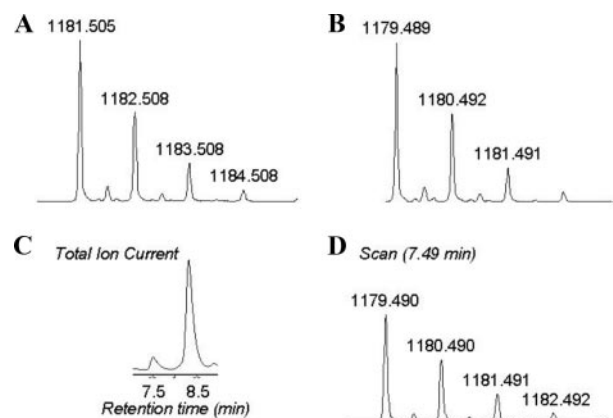 accompanies oxidation of EcDsbA and NmDsbA3. Progress curves are shown for the reoxidation of EcDsbA (50 μM) (■) and NmDsbA3 (50 μM) (▲) by EcDsbB (80 nM). In the absence of EcDsbB there is no change in fluorescence for either EcDsbA (▼) or NmDsbA3 (data not shown). Both EcDsbA and NmDsbA3 are substrates for EcDsbB and are reoxidized at a similar rate. *C* and *D*, disulfide oxidase activity was determined by monitoring the oxidation of a model peptide substrate derived from the *Neisserial* pilin subunit PilE. The kinetics of the oxidation reactions were determined using stopped-flow fluorescence by monitoring the increase in fluorescence upon reduction of DsbA in the assay. Both EcDsbA and NmDsbA3 catalyze the oxidation of the PilE peptide, with NmDsbA3 being the more efficient catal.
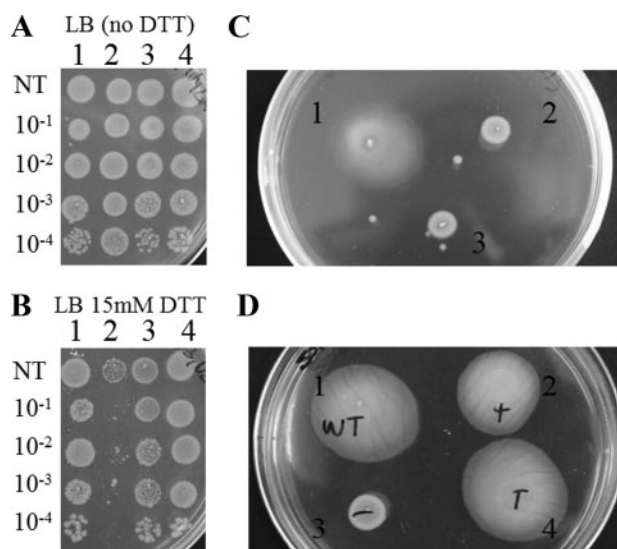
FIGURE 7. **Complementation assays.** *A* and *B*, wild type *E. coli* JCB570 (*lane 1*) were able to grow in the presence of DTT (15 mM), whereas the corresponding *dsbA*-null strain JCB571 (*lane 2*) were not. Expression of EcDsbA (*lane 3*) or NmDsbA3 (*lane 4*) from the high copy expression plasmid ptrc99A restored resistance to DTT in JCB571. *C*, expression of EcDsbA from the low copy vector pHSG576 restored motility to JCB571 (*zone 1*). In contrast, expression of NmDsbA3 from pHSG576 (*zone 3*) did not restore motility. JCB571 containing the empty expression vector (*zone 2*) was non-motile. *D*, motility was restored to JCB571 when EcDsbA (*zone 2*) and NmDsbA3 (*zone 4*) were expressed from the high copy expression vector, ptrc99A. JCB571 containing the empty pTrc99A was non-motile (*zone 3*). JCB570 is a motile positive control (*zone 1*).

dation of DsbA. This assay revealed that NmDsbA3 is a substrate for EcDsbB (Fig. 5*B*). The rates of oxidation of NmDsbA3 and EcDsbA in this assay were similar, suggesting that NmDsbA3 is a substrate for EcDsbB and may be reoxidized by EcDsbB *in vivo*.

Functional Studies—We then wished to explore further the functional role of NmDsbA3 *in vivo*. The *E. coli* *dsbA* mutant strain JCB571 is sensitive to DTT and is not motile on soft agar due to a disulfide bond deficiency in FlgI, a component of the flagellum motor. The ability of NmDsbA3 to complement JCB571 resistance to DTT and motility was assessed. Previously, complementation studies have been reported for JCB571 transformed with a vector containing NmdsbA3 in pGEM-T (16). The transformed cells were demonstrated to express NmDsbA3 to the periplasm. The level of expression of NmDsbA3 was similar to that of EcDsbA expressed from the same vector, but whereas EcDsbA complemented JCB571, expression of NmDsbA3 had no effect on either motility or DTT resistance (16). We observed similar results in JCB571 when NmDsbA3 and EcDsbA were expressed from the low expression vector pHSG576. To determine whether higher expression levels of NmDsbA3 would result in complementation of JCB571, NmDsbA3 was expressed from the high expression vector pTrc99A. Expression of NmDsbA3 from a high copy vector in the transformed JCB571 strain CKEC293 conferred resistance to DTT (15 mM) and motility on 0.4% LB agar similar to the positive control strain CKEC289 expressing the EcDsbA and wild-type strain JCB570 (Fig. 7, *A* and *B*). Similar results for CKEC293 were obtained when assays were repeated in the presence of isopropyl 1-thio-β-ᴅ-galactopyranoside (data not shown). Thus, NmDsbA3 also functions as an oxi-

doreductase *in vivo*, albeit with an apparently reduced activity in comparison to EcDsbA.

DISCUSSION

It has previously been demonstrated that *N. meningitidis* expressing NmDsbA3 in the absence of NmDsbA1 and NmDsbA2 are sensitive to DTT and do not express functional pili (4). Furthermore, NmDsbA3 was previously found to be unable to complement the non-motile phenotype of *dsbA*-null *E. coli* (16). From these findings it has been inferred that NmDsbA3 has a limited repertoire and does not oxidize a wide range of substrate proteins found in the periplasm of *N. meningitidis* and *E. coli*.

To begin to address the apparent atypical function of NmDsbA3, we determined its structure and undertook a series of functional studies. The structure revealed that NmDsbA3 possessed a DsbA-like fold, and displayed oxidoreductase activities typical of the DsbA family. Interestingly, the structure of NmDsbA3 revealed a number of distinct features that may be critical in dictating the observed activity of the enzyme. Several of the differences between the structure of NmDsbA3 and EcDsbA are found in the key loops that surround the active site of the enzyme. These include the first loop connecting the thioredoxin and helical domains as well as the *cis*-Pro loop. Notably NmDsbA1 and NmDsbA2, which share 78% sequence identity, have been demonstrated to have different activities *in vivo*, but have divergent sequences in both of these loops. It has previously been demonstrated that mutations in the *cis*-Pro loop of DsbC and DsbG can affect the substrate specificity of these enzymes (38). Thus, it is possible that the sequence of the *cis*-Pro loop is critical in dictating the substrate repertoire of Dsb enzymes. To illustrate, most Gram-negative DsbA enzymes have a Val residue preceding the *cis*-Pro that is located adjacent to the active site. Although the structure of NmDsbA3 retains the *cis*-Pro, the residue preceding it is Thr. A similar motif (Thr-*cis*-Pro) is highly conserved in Gram-negative disulfide isomerases (DsbC and DsbG). The Thr-*cis*-Pro sequence that is present in NmDsbA3 raises the question of whether it acts as oxidase or isomerase. Our *in vitro* measurements of the oxidoreductase activity of NmDsbA3 suggests that it is an oxidase rather than an isomerase. A Thr-*cis*-Pro sequence has previously been reported in the Gram-positive DsbA from *Staphylococcus aureus* (SaDsbA), which is also a disulfide oxidase *in vivo*. There are a number of differences between SaDsbA and the DsbA enzymes of Gram-negative bacteria, notably that the disulfide bond does not destabilize the oxidized form of the protein (39) in contrast to EcDsbA (40) and VcDsbA (41), and *S. aureus* does not possess a DsbB ortholog, suggesting that it is oxidized by a different mechanism to that observed in Gram-negative bacteria. Notwithstanding these differences, SaDsbA displays *in vitro* activity that is reminiscent of an oxidase rather than an isomerase (39). Furthermore, both NmDsbA1 and NmDsbA2, each of which are capable of partially complementing *dsbA*-null *E. coli* (4, 16), and therefore most likely act as oxidase enzymes *in vivo* retain the Thr-*cis*-Pro motif that is present in NmDsbA3. This is consistent with the view that the sequence of the *cis*-Pro loop is critical in determining substrate

specificity, but does not necessarily dictate the oxidase or isomerase activity of the enzyme (38, 39).

Despite the differences in the loop sequences that surround the active site, a number of the conserved surface features that have been observed in other DsbA enzymes (37) also appear to be present in NmDsbA3. Both the hydrophobic patch (Fig. 4) and the hydrophobic groove adjacent to the active site are conserved in the structure of NmDsbA3. The hydrophobic groove, which forms the binding site in EcDsbA for EcDsbB, is shortened in NmDsbA3. There are similar deletions in both VcDsbA and SaDsbA, which also result in a shortening of helix $\alpha 7$. However, the electrostatic surfaces of the proteins are quite different. In EcDsbA, VcDsbA, and NmDsbA, the groove has a hydrophobic surface, whereas in SaDsbA the groove is charged (39). We have determined that NmDsbA3 is re-oxidized by EcDsbB *in vitro* and at a similar rate to EcDsbA. Furthermore, because VcDsbA complements the motility of *dsbA*-null *E. coli*, it is also presumed to be a substrate for EcDsbB. In contrast, it has been shown the SaDsbA is not a substrate for EcDsbB (39). Thus it appears that the nature of the surface, rather than the length of helix $\alpha 7$ *per se* is the important determinant of specificity for EcDsbB.

However, these differences in the nature of the groove cannot fully explain the observed activities of the different DsbA enzymes. For example, SaDsbA appears to be more like EcDsbA, in that it can complement *dsbA*-null *E. coli* and is capable of restoring the motility, whereas NmDsbA3 can only do so when it is strongly overexpressed. In contrast, NmDsbA3 and EcDsbA show similar activity toward EcDsbB and both are capable of catalyzing the reduction of insulin, whereas SaDsbA is not reoxidized by EcDsbB and does not catalyze insulin reduction (39, 42). Finally, *dsbA*-null *E. coli* display pleiotropic phenotypes associated with a deficiency in oxidative protein folding (5, 6, 12), whereas, deletion of either *SadsbA* or *NmdsbA3* from their respective hosts does not produce any measurable phenotype either *in vitro* or *in vivo* (4, 16, 42). Taken together, these observations suggest that NmDsbA3 and SaDsbA have a narrower substrate repertoire than EcDsbA. Furthermore, they indicate that disulfide oxidase activity can be maintained in DsbA enzymes that are not substrates for EcDsbB, which may indicate that the processes by which oxidized DsbA recognizes its substrates are subtly different from those that dictate the interation of reduced DsbA with DsbB.

The structures of NmDsbA3 and SaDsbA provide a rationale for these observations. Despite retaining a similar fold to EcDsbA, there are a number of critical differences between the structures of different DsbA enzymes. The hydrophobic groove, which is absent in SaDsbA appears to be essential for interaction with EcDsbB. In contrast, the hydrophobic groove is not an absolute requirement for oxidase activity, but changes in the composition and conformation of the surface loops that surround the active site appear to regulate interaction with substrates. One of these loops contains the conserved *cis*-Pro residue that is common to all thioredoxin-like proteins and has previously been shown to regulate substrate specificity in disulfide isomerases DsbC and DsbG (38). Taken together these findings suggest that this may be a common mechanism for regulating the specificity of thioredoxin-fold oxidoreductases.

REFERENCES

1. Stephens, D. S., Greenwood, B., and Brandtzaeg, P. (2007) *Lancet* **369,** 2196–2210
2. Stephens, D. S., and McGee, Z. A. (1981) *J. Infect. Dis.* **143,** 525–532
3. Bourdoulous, S., and Nassif, X. (2006) in *Handbook of Meningococcal Disease* (Frosch, M., and Maiden, M. C. J., eds) WILEY-VCH Verlag GmbH & Co, Weiheim, Germany
4. Tinsley, C. R., Voulhoux, R., Beretti, J. L., Tommassen, J., and Nassif, X. (2004) *J. Biol. Chem.* **279,** 27078–27087
5. Akiyama, Y., Kamitani, S., Kusukawa, N., and Ito, K. (1992) *J. Biol. Chem.* **267,** 22440–22445
6. Bardwell, J. C., McGovern, K., and Beckwith, J. (1991) *Cell* **67,** 581–589
7. Missiakas, D., Georgopoulos, C., and Raina, S. (1993) *Proc. Natl. Acad. Sci. U. S. A.* **90,** 7084–7088
8. Missiakas, D., Georgopoulos, C., and Raina, S. (1994) *EMBO J.* **13,** 2013–2020
9. Missiakas, D., Schwager, F., and Raina, S. (1995) *EMBO J.* **14,** 3415–3424
10. Peek, J. A., and Taylor, R. K. (1992) *Proc. Natl. Acad. Sci. U. S. A.* **89,** 6210–6214
11. Nakamoto, H., and Bardwell, J. C. (2004) *Biochim. Biophys. Acta* **1694,** 111–119
12. Dailey, F. E., and Berg, H. C. (1993) *Proc. Natl. Acad. Sci. U. S. A.* **90,** 1043–1047
13. Hizukuri, Y., Yakushi, T., Kawagishi, I., and Homma, M. (2006) *J. Bacteriol.* **188,** 4190–4197
14. Kadokura, H., Tian, H., Zander, T., Bardwell, J. C., and Beckwith, J. (2004) *Science* **303,** 534–537
15. Sinha, S., Ambur, O. H., Langford, P. R., Tonjum, T., and Kroll, J. S. (2008) *Microbiology* **154,** 217–225
16. Sinha, S., Langford, P. R., and Kroll, J. S. (2004) *Microbiology* **150,** 2993–3000
17. Sambrook, J., Fritch, E. F., and Maniatis, T. (1989) *Molecular Cloning: A Laboratory Manual*, Cold Spring Harbor Laboratory, Cold Spring Harbor, NY
18. Takeshita, S., Sato, M., Toba, M., Masahashi, W., and Hashimoto-Gotoh, T. (1987) *Gene (Amst.)* **61,** 63–74
19. Chung, C. T., and Miller, R. H. (1988) *Nucleic Acids Res.* **16,** 3580
20. Martin, J. L., Waksman, G., Bardwell, J. C., Beckwith, J., and Kuriyan, J. (1993) *J. Mol. Biol.* **230,** 1097–1100
21. Studier, F. W. (2005) *Protein Expression Purif.* **41,** 207–234
22. Marley, J., Lu, M., and Bracken, C. (2001) *J. Biomol. NMR* **20,** 71–75
23. Otwinowski, Z., and Minor, W. (1997) *Methods Enzymol.* **276,** 307–326
24. Terwilliger, T. C., and Berendzen, J. (1999) *Acta Crystallogr. Sect. D Biol. Crystallogr.* **55,** 849–861
25. Collaborative Computational Project Number 4 (1994) *Acta Crystallogr. Sect. D Biol. Crystallogr.* **50,** 760–763
26. Vagin, A. A., and Isupov, M. N. (2001) *Acta Crystallogr. Sect. D Biol. Crystallogr.* **57,** 1451–1456
27. Hu, S. H., Peek, J. A., Rattigan, E., Taylor, R. K., and Martin, J. L. (1997) *J. Mol. Biol.* **268,** 137–146
28. Emsley, P., and Cowtan, K. (2004) *Acta Crystallogr. Sect. D Biol. Crystallogr.* **60,** 2126–2132
29. Murshudov, G. N., Vagin, A. A., and Dodson, E. J. (1997) *Acta Crystallogr. Sect. D Biol. Crystallogr.* **53,** 240–255
30. Holmgren, A. (1979) *J. Biol. Chem.* **254,** 9627–9632
31. Bader, M., Muse, W., Zander, T., and Bardwell, J. (1998) *J. Biol. Chem.* **273,** 10302–10307

32. Sardesai, A. A., Genevaux, P., Schwager, F., Ang, D., and Georgopoulos, C. (2003) *EMBO J.* **22,** 1461–1466

33. Macnab, R. M. (1986) *Methods Enzymol.* **125,** 563–581

34. Martin, J. L., Bardwell, J. C., and Kuriyan, J. (1993) *Nature* **365,** 464–468

35. Martin, J. L. (1995) *Structure* **3,** 245–250

36. Inaba, K., Murakami, S., Suzuki, M., Nakagawa, A., Yamashita, E., Okada, K., and Ito, K. (2006) *Cell* **127,** 789–801

37. Guddat, L. W., Bardwell, J. C., Zander, T., and Martin, J. L. (1997) *Protein Sci.* **6,** 1148–1156

38. Hiniker, A., Ren, G., Heras, B., Zheng, Y., Laurinec, S., Jobson, R. W., Stuckey, J. A., Martin, J. L., and Bardwell, J. C. (2007) *Proc. Natl. Acad. Sci. U. S. A.* **104,** 11670–11675

39. Heras, B., Kurz, M., Jarrott, R., Shouldice, S. R., Frei, P., Robin, G., Cemazar, M., Thony-Meyer, L., Glockshuber, R., and Martin, J. L. (2008) *J. Biol. Chem.* **283,** 4261–4271

40. Zapun, A., Bardwell, J. C., and Creighton, T. E. (1993) *Biochemistry* **32,** 5083–5092

41. Horne, J., d'Auvergne, E. J., Coles, M., Velkov, T., Chin, Y., Charman, W. N., Prankerd, R., Gooley, P. R., and Scanlon, M. J. (2007) *J. Mol. Biol.* **371,** 703–716

42. Dumoulin, A., Grauschopf, U., Bischoff, M., Thony-Meyer, L., and Berger-Bachi, B. (2005) *Arch. Microbiol.* **184,** 117–128

Structural and Biochemical Characterization of the Oxidoreductase NmDsbA3 from *Neisseria meningitidis*

Julian P. Vivian, Jessica Scoullar, Amy L. Robertson, Stephen P. Bottomley, James Horne, Yanni Chin, Jerome Wielens, Philip E. Thompson, Tony Velkov, Susannah Piek, Emma Byres, Travis Beddoe, Matthew C. J. Wilce, Charlene M. Kahler, Jamie Rossjohn and Martin J. Scanlon

Access the most updated version of this article at doi: 10.1074/jbc.M803990200

Alerts:

- When this article is cited
- When a correction for this article is posted

Click here to choose from all of JBC's e-mail alerts

This article cites 40 references, 13 of which can be accessed free at
http://www.jbc.org/content/283/47/32452.full.html#ref-list-1